ICAP-1 monoubiquitylation coordinates matrix density and rigidity sensing for cell migration through ROCK2–MRCKα balance

Anne-Pascale Bouin, Alexander Kyurmurkov, Myriam Régent-Kloeckner, Anne-Sophie Ribba, Eva Faurobert, Henri-Noël Fournier, Ingrid Bourrin-Reynard, Sandra Manet-Dupé, Christiane Oddou, Martial Balland, et al.

The Company of Biologists

RESEARCH ARTICLE

ICAP-1 monoubiquitylation coordinates matrix density and rigidity sensing for cell migration through ROCK2–MRCKα balance

Anne-Pascale Bouin[1,2,3], Alexander Kyurmurkov[1,2,3], Myriam Régent-Kloeckner[1,2,3,*], Anne-Sophie Ribba[1,2,3], Eva Faurobert[1,2,3], Henri-Noël Fournier[1,2,3], Ingrid Bourrin-Reynard[1,2,3], Sandra Manet-Dupé[1,2,3], Christiane Oddou[1,2,3], Martial Balland[3,4], Emmanuelle Planus[1,2,3] and Corinne Albiges-Rizo[1,2,3,‡]

ABSTRACT

Cell migration is a complex process requiring density and rigidity sensing of the microenvironment to adapt cell migratory speed through focal adhesion and actin cytoskeleton regulation. ICAP-1 (also known as ITGB1BP1), a β1 integrin partner, is essential for ensuring integrin activation cycle and focal adhesion formation. We show that ICAP-1 is monoubiquitylated by Smurf1, preventing ICAP-1 binding to β1 integrin. The non-ubiquitylatable form of ICAP-1 modifies β1 integrin focal adhesion organization and interferes with fibronectin density sensing. ICAP-1 is also required for adapting cell migration in response to substrate stiffness in a β1-integrin-independent manner. ICAP-1 monoubiquitylation regulates rigidity sensing by increasing MRCKα (also known as CDC42BPA)-dependent cell contractility through myosin phosphorylation independently of substrate rigidity. We provide evidence that ICAP-1 monoubiquitylation helps in switching from ROCK2-mediated to MRCKα-mediated cell contractility. ICAP-1 monoubiquitylation serves as a molecular switch to coordinate extracellular matrix density and rigidity sensing thus acting as a crucial modulator of cell migration and mechanosensing.

KEY WORDS: Cell migration, Rigidity sensing, ICAP-1, Integrin, Monoubiquitylation, Cell contractility

INTRODUCTION

Motile cells continuously sample in space and time the heterogeneity in the composition and stiffness of their extracellular matrix (ECM) through integrin-mediated focal adhesions (FAs) (Moore et al., 2010). As a mechanical link between ECM and actin stress fibers, integrins are crucial for force transmission and signal transduction (Moore et al., 2010). FA assembly, growth and maintenance depend on actomyosin traction forces, which adapt to the substrate elasticity (Burridge and Wittchen, 2013). In spite of alternative pathways involving MRCK (which has two isoforms, MRCKα and MRCKβ, also known as CDC42BPA and CDC42BPB, respectively), MLCK (also known as MYLK) or mDia (Burridge and Wittchen, 2013; Chen et al., 2014; Jégou et al., 2013; Totsukawa et al., 2004), a key event is the modulation of cellular contractility through myosin-based contractility and ROCK (which has two isoforms, ROCK1 and

ROCK2) activity. However, signaling pathways underlying FA-mediated rigidity sensing and the mechano-response are not fully understood.

ICAP-1 (also known as ITGB1BP1), a negative regulator of β1 integrin, enables the cell to sense ECM density to adapt its adhesive and migratory responses (Millon-Frémillon et al., 2008) and to control fibronectin (FN) remodeling (Brunner et al., 2011; Faurobert et al., 2013). ICAP-1 specifically binds to the cytoplasmic tail of β1 integrin, maintaining the integrin in its inactivated form by competing with the two activators named Kindlin and talin (Brunner et al., 2011; Millon-Frémillon et al., 2008; Montanez et al., 2008; Ye et al., 2014). ICAP-1 also binds to ROCK1 (Peter et al., 2006). Thanks to these interactions, ICAP-1 may be a good candidate for regulating myosin-based contractility and cellular response to ECM stiffness. Tunable post-translational modifications may control ICAP-1 functions enabling the cell to adapt its migratory response. As ubiquitylation is emerging as important for cell migration dynamics and cell contractility (Carvallo et al., 2010; Sahai et al., 2007; Schaefer et al., 2012; Su et al., 2013; Wang et al., 2003), we addressed whether ubiquitylation may control ICAP-1 functions, enabling the cell to adapt its migratory response. Here, we show that ICAP-1 is monoubiquitylated by SMAD ubiquityl regulatory factor 1 (Smurf1). This monoubiquitylation impairs ICAP-1 binding to β1 integrin and is involved in ECM density and rigidity sensing as well as in coordination of the dynamics of adhesion sites and contractile machinery. ICAP-1 monoubiquitylation plays an important role in the responses of migrating cells to mechanical inputs in a β1 integrin-independent manner by promoting the switch from a ROCK2-mediated to an MRCKα-mediated contractility pathway.

RESULTS

ICAP-1 is monoubiquitylated by Smurf1 at the β1 integrin-binding site

To investigate ICAP-1 ubiquitylation, we performed nickel-bead pulldown experiments on Chinese Hamster Ovary (CHO) cells transfected with ICAP-1 either in the presence or absence of co-transfection with His-tagged ubiquitin. The proteasome inhibitor MG132 was added to prevent proteasomal degradation of any ubiquitylated ICAP-1. When expressed alone, ICAP-1 appeared on a western blot an apparent molecular mass that was slightly greater than 20 kDa, whereas co-transfection with His-tagged ubiquitin and pulldown on nickel beads resulted in isolation of ICAP-1 with higher molecular mass forms, with a band above 35 kDa (Fig. 1A), showing that ICAP-1 is indeed ubiquitylated. This band above 35 kDa most likely corresponds to ICAP-1 monoubiquitylation. HA-tagged ubiquitin (HA–Ubi) was also coexpressed with ICAP-1 fused to Flag and our results show that ICAP-1–Flag can be recognized by both anti-Flag and anti-HA antibodies after immunoprecipitation with anti-Flag antibodies (Fig. 1B),
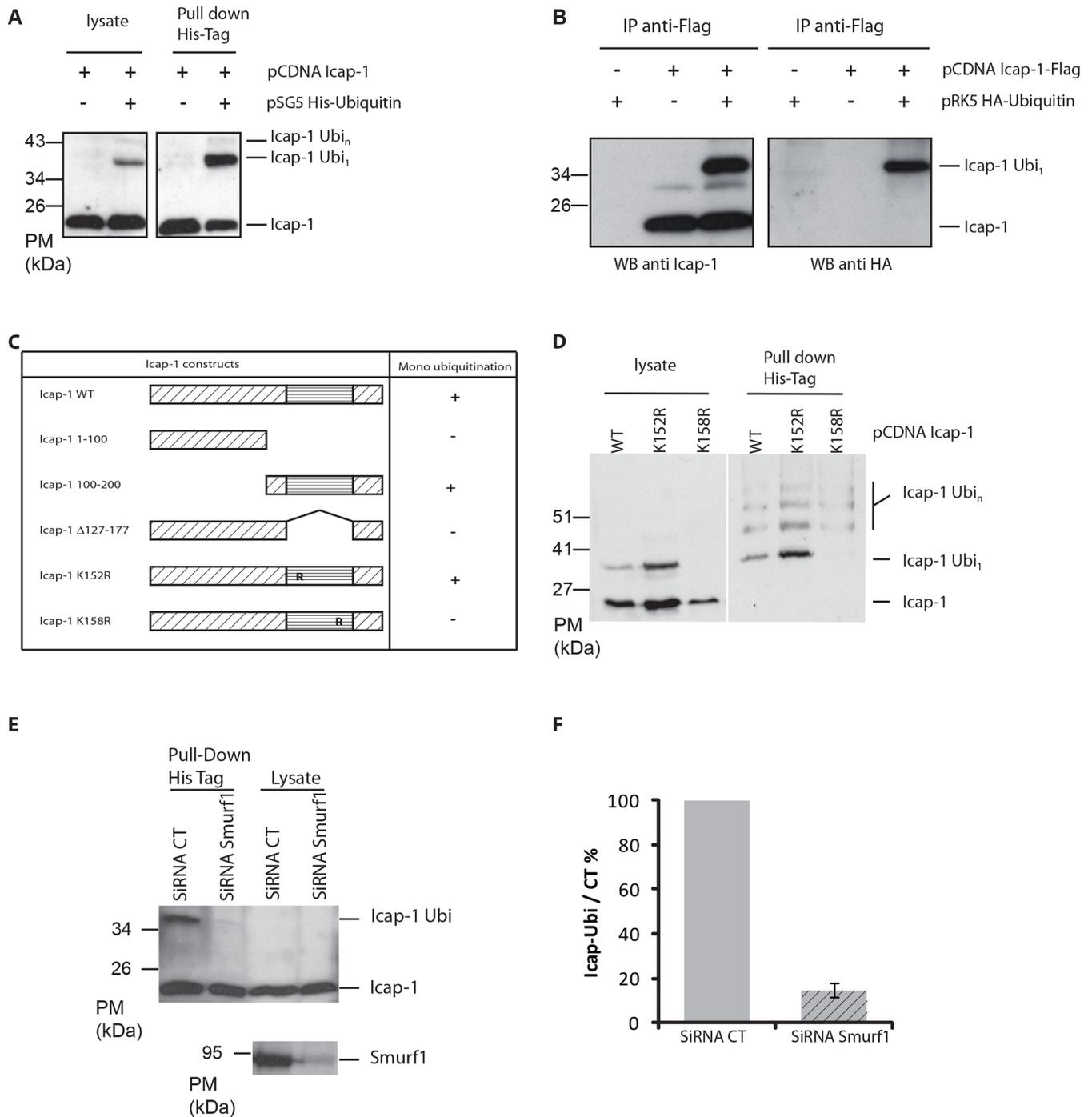
Journal of Cell Science

Fig. 1. The Smurf1 ubiquitin ligase is responsible for ICAP-1 monoubiquitylation. (A) ICAP-1 was overexpressed in CHO cells with or without His-tagged ubiquitin. After pulldown on TALON resin, the ubiquitylated proteins were analyzed by western blotting with the anti-ICAP-1 antibody. ICAP-1 was monoubiquitylated (Icap-1 Ubi_1) and weakly polyubiquitylated (Icap-1 Ubi_n). (B) ICAP-1–Flag immunoprecipitated by anti-Flag antibody can be recognized by anti-HA antibodies (as assessed by western blotting) after co-transfection with HA–Ubi and ICAP-1–Flag in CHO cells. The results are representative of more than three independent experiments. (C) Different ICAP-1 constructs were used to identify the ubiquitylated lysine residue. The horizontal-striped box corresponds to the β1 integrin-binding site. (D) ICAP-1 WT, ICAP-1 K152R or ICAP-1 K158R were overexpressed in CHO cells with His-tagged ubiquitin. His-tagged pulldown assays show that only the ICAP-1 K158R mutant was not monoubiquitylated. The results are representative of three independent experiments. (E) HeLa cells with or without Smurf1 knockdown were co-transfected with ICAP-1 and His-tagged ubiquitin. After pulldown on TALON resin, the ubiquitylated proteins were analyzed by western blotting with the anti-ICAP-1 antibody. Non-ubiquitylated ICAP-1 was used to ensure equivalent ICAP-1 levels in both lysates. CT, control. (F) Quantification of the level of ubiquitylated ICAP-1 in Smurf1-silenced HeLa cells. Error bars represent s.e.m. (*n*=3). PM, position of molecular mass makers.

confirming that ICAP-1 can be ubiquitylated. Furthermore, to identify which lysine residue is monoubiquitylated, we analyzed whether truncated forms of ICAP-1 could be monoubiquitylated (Fig. 1C). We determined that the monoubiquitylation site was

located in the binding domain for β1 integrin. The point mutation of either one of the two lysine residues present in this domain identified lysine K158 as the site of monoubiquitylation, as its replacement with arginine led to the absence of the 35 kDa band

(Fig. 1D) without changing the ICAP-1 polyubiquitylation states (Fig. 1D). The non-ubiquitylable K158R mutant was even less stable than wild-type (WT) ICAP-1, suggesting that the monoubiquitylated form of ICAP-1 is not targeted for proteasomal degradation but rather may have a signaling function (Fig. S1A,B). Because Smurf1 catalyzes the ubiquitylation of the integrin activator talin (Huang et al., 2009), we hypothesized that Smurf1 could be responsible for ICAP-1 monoubiquitylation. To test this hypothesis, Smurf1 was silenced by small interfering RNA (siRNA); there was a high efficiency in reducing Smurf1 transcript and protein levels without affecting ICAP-1 expression (Fig. 1E). ICAP1 monoubiquitylation was blocked when Smurf1 was knocked down, suggesting that Smurf1 is necessary for promoting ICAP-1 monoubiquitylation (Fig. 1E,F). A pulldown assay shows that purified recombinant Smurf1–GST is able to bind to exogenously expressed ICAP-1 in CHO cells, in contrast to the null interaction with GST alone (50-fold less) or with the weak binding to GST fused to Smurf2 (10-fold less) (Fig. S1C). Smurf2 had been chosen as a control because overlapping but distinct substrate and regulator specificity has been observed between Smurf1 and Smurf2 (Lu et al., 2008, 2011). The co-immunoprecipitation between Smurf1–Myc and ICAP-1–Flag expressed in CHO cells confirms that Smurf1 and ICAP-1 belong to the same complex (Fig. S1D). A direct interaction between Smurf1 and ICAP-1 was demonstrated by an ELISA assay using purified recombinant GST–Smurf1 and purified recombinant ICAP-1–His (Fig. S1E). Taken together, our results indicate that Smurf1 is responsible for ICAP-1 monoubiquitylation.

The monoubiquitylation of ICAP-1 prevents binding to β1 integrin and regulates β1 integrin-dependent adhesion

According to structure predictions and crystallographic data (Chang et al., 2002; Liu et al., 2013), the monoubiquitylation site is located in the β1 integrin-binding domain of ICAP-1 facing the isoleucine residue important for the binding to β1 integrin (Fig. 2A). As this monoubiquitylation could interfere with the interaction between ICAP-1 and β1 integrin, we used two classical methods to produce an ubiquitylated form of a protein (Torrino et al., 2011; Visvikis et al., 2008), first by co-transfecting ICAP-1 with His-tagged ubiquitin and second by creating a chimera made of ubiquitin fused to the C-terminal tail of ICAP-1 (ICAP-1–Ubi) (Fig. 2B). We tested the ability of WT, non-ubiquitylatable (K158R) and monoubiquitylated ICAP-1 (endogenous ubiquitylation or chimera) to interact with the cytoplasmic domain of either β1 integrin or β3 integrin fused with GST or with GST alone by pulldown assay (Fig. S2A) or by ELISA assay (Fig. 2C). As previously reported (Millon-Frémillon et al., 2008), we confirmed that ICAP-1 specifically interacts with the cytoplasmic domain of β1 integrin (Fig. 2C; Fig. S2A). Furthermore, the non-ubiquitylated K158R mutant retained the ability to interact with the cytoplasmic domain of β1 integrin, whereas both ubiquitylated forms of ICAP-1 (His-tagged and chimeric) lost the capacity to interact with the cytoplasmic domain of β1 integrin (Fig. 2C; Fig. S2A). These results show that ICAP-1 monoubiquitylation prevents the interaction of ICAP-1 with β1 integrin.

Next, we investigated whether the monoubiquitylation of ICAP-1 could affect FA organization by rescuing ICAP-1-deficient osteoblast cells with a similar stable expression of WT ICAP-1, non-ubiquitylatable ICAP-1 K158R and of the chimeric ubiquitylated form. All osteoblast cell lines were able to spread onto FN and develop FAs containing β1 integrins, as revealed by 9EG7 antibody staining for activated β1 integrin (Fig. 2D). Like ICAP-1-deficient

cells, cells expressing the ubiquitylated form of ICAP-1 displayed more numerous β1 integrin-containing FAs compared with cells expressing the WT form (Fig. 2D–F) because of the inability of the monoubiquitylated ICAP-1 to inhibit β1 integrin. Conversely, cells expressing the non-ubiquitylatable ICAP-1 K158R mutant displayed fewer, smaller and more-punctate adhesion sites (Fig. 2D–F) compared with those of WT ICAP-1, likely due to its ability to interact with β1 integrin and thus inhibit the assembly of larger FAs (Bouvard et al., 2007; Millon-Frémillon et al., 2008).

As Smurf1 is responsible for ICAP-1 monoubiquitylation, we investigated whether the formation of β1 integrin-containing FAs was dependent on Smurf1 activity. As expected, the deletion of Smurf1 led to a decrease in the number and area of β1 integrin-containing FA (Fig. S2B,C,D) phenocopying the non-ubiquitylatable ICAP-1 K158R phenotype (Fig. 2D–F). Conversely, the ubiquitylated ICAP-1 was able to bypass the destructive effect of Smurf1 deletion on β1 integrin-containing FAs (Fig. S2B,C,D). Thus, Smurf-1-mediated ICAP-1 monoubiquitylation plays a crucial role in the organization of β1 integrin-containing FA by preventing or disrupting the ICAP-1–β1-integrin interaction.

ICAP-1 monoubiquitylation is a signal coordinating FN density sensing with rigidity sensing

We wondered whether ICAP-1 monoubiquitylation was involved in FN density and rigidity sensing. To test an effect on FN density sensing, single-cell tracking of sparse cells was performed to monitor the migration speed of ICAP-1-deficient osteoblast or mouse embryonic fibroblast (MEF) cells expressing WT ICAP-1, K158R ICAP-1 or ICAP-1–Ubi in the presence of increasing concentrations of FN. As expected (Discher et al., 2005; Engler et al., 2006; Raab et al., 2012), WT ICAP-1-expressing osteoblasts (Fig. 3A; Movies 1,2) or MEFs (Fig. S3A) displayed faster migration rates with increasing FN density. While the migratory speed of the cells expressing the ubiquitylated ICAP-1 form depended on ECM density, like ICAP-1 null cells, the cells expressing the non-ubiquitylatable K158R mutant maintained the same migration speed whatever the density of FN coating (Fig. 3A; Fig. S3A, Movies 3,4). Moreover, the ability to adapt their migration response to ECM density was lost in cells treated with siRNA against Smurf1 but was rescued in cells co-expressing the monoubiquitylated ICAP-1 showing that the Smurf1-dependent monoubiquitylation of ICAP-1 is necessary for cells to sense and respond to FN density (Fig. S3B).

To explore the possibility that the inability of the K158R mutant to adapt its migration speed to FN density could be due to a greater capacity to lock β1 integrin in its inactivated form than with WT ICAP-1, we analyzed the response of cells treated with β1 integrin-blocking antibodies to increasing FN density. We showed that these cells were unable to sense the density of FN or adapt their migratory behavior (Fig. 3B), confirming the requirement for β1 integrin activation for the adaptation of the cell migration rate to the FN density. Additionally, cells co-expressing a β1 integrin mutant that lacks ICAP-1 binding (β1 V787T) with the ICAP-1 K158R mutant or in the context of silenced Smurf1 were still able to adapt their migration speed to the FN density (Fig. 3B; Fig. S3C). Therefore, the unresponsiveness of cells to the FN density is most likely due to the inhibitory interaction between the non-ubiquitylatable ICAP-1 and β1 integrin. Overall, ICAP-1 monoubiquitylation by Smurf1 is required to release ICAP-1 inhibitory effect on β1 integrin in order to permit the adaptation of cell migration to ECM density.
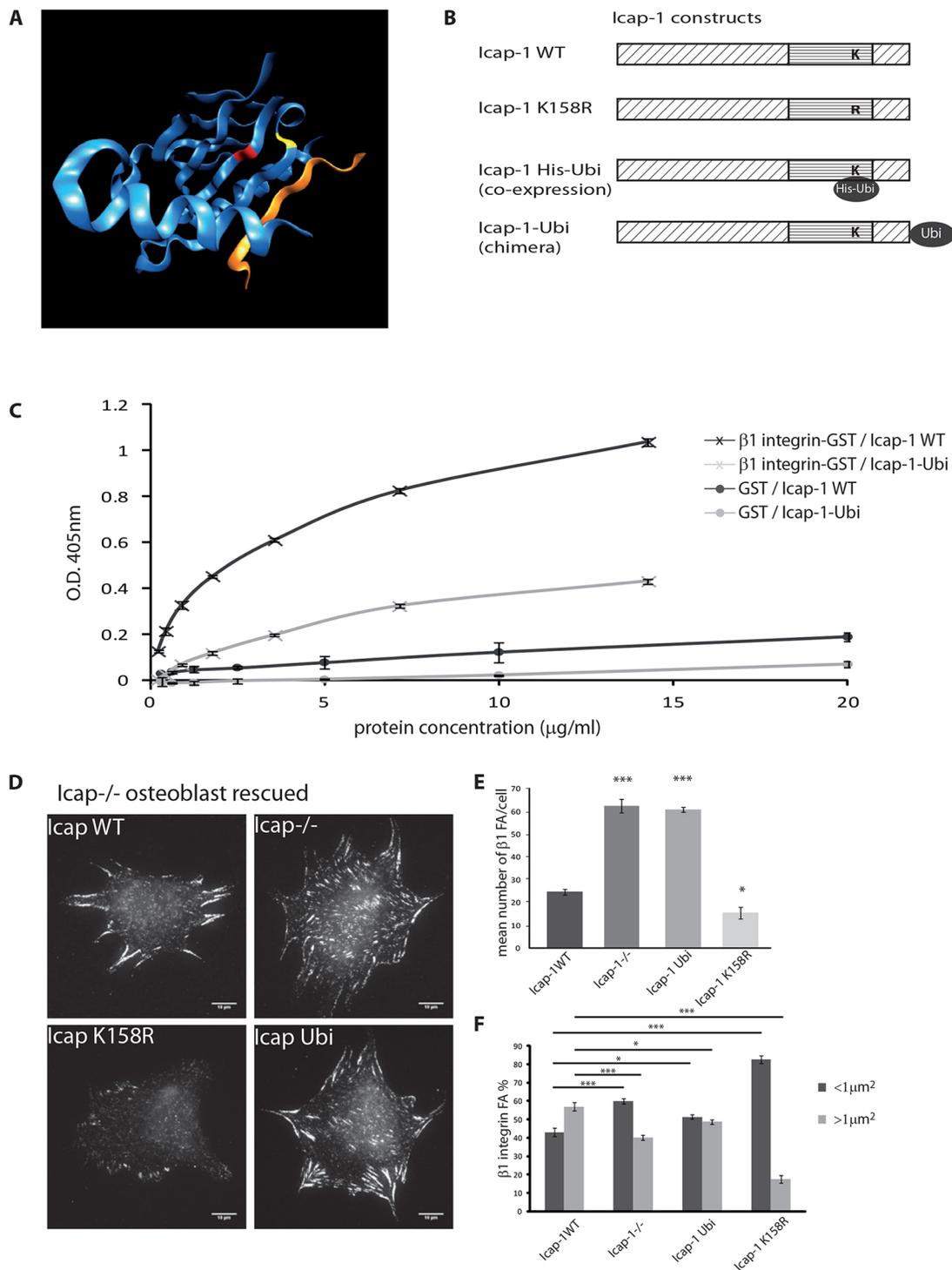
Fig. 2. Ubiquitylated ICAP-1 does not interact with the β1 integrin cytoplasmic tail and disorganizes FA distribution. (A) Recently published structure of ICAP-1 interacting with the β1 integrin cytoplasmic tail (PDB 4DX9) (Liu et al., 2013). Blue, ICAP-1 protein with I139 represented in yellow and K158 represented in red. Orange, β1 integrin cytoplasmic tail. This image was made with VMD, NAMD, BioCoRE, JMV and other software support (these software packages are developed with NIH support by the Theoretical and Computational Biophysics group at the Beckman Institute, University of Illinois at Urbana-Champaign). (B) ICAP-1 constructs used for the study. K158R is the non-ubiquitylatable form. ICAP-1–His–Ubi results from the overexpression of ICAP-1 and His-tagged ubiquitin proteins in CHO cells. ICAP-1–Ubi is a chimeric form with ubiquitin fused at the C-terminus of ICAP-1 to mimic constitutive monoubiquitylation. (C) Interaction between recombinant ICAP-1–His or ICAP-1–Ubi–His and recombinant GST or the GST–β1 integrin cytoplasmic domain as determined by an ELISA assay. The results are representatives of three independent experiments. (D) β1 integrin staining in ICAP-1-null osteoblasts or ICAP-1-null cells rescued with ICAP-1 WT, non-ubiquitylatable ICAP-1 or the ICAP-1 ubiquitin chimera spread on FN for 2.5 h. The cells expressing the non-ubiquitylatable form (K158R) display smaller β1 integrin FAs compared with the cells expressing ICAP-1 WT. Scale bars: 10 μm. (E) Quantification of the β1 integrin focal adhesion number and (F) distribution of the β1 integrin focal adhesion areas. Analyses were performed on 30–40 cells from two independent experiments. Error bars indicate s.e.m. *$P<0.05$, ***$P<0.0005$ (one-way ANOVA and Tukey's HSD test).
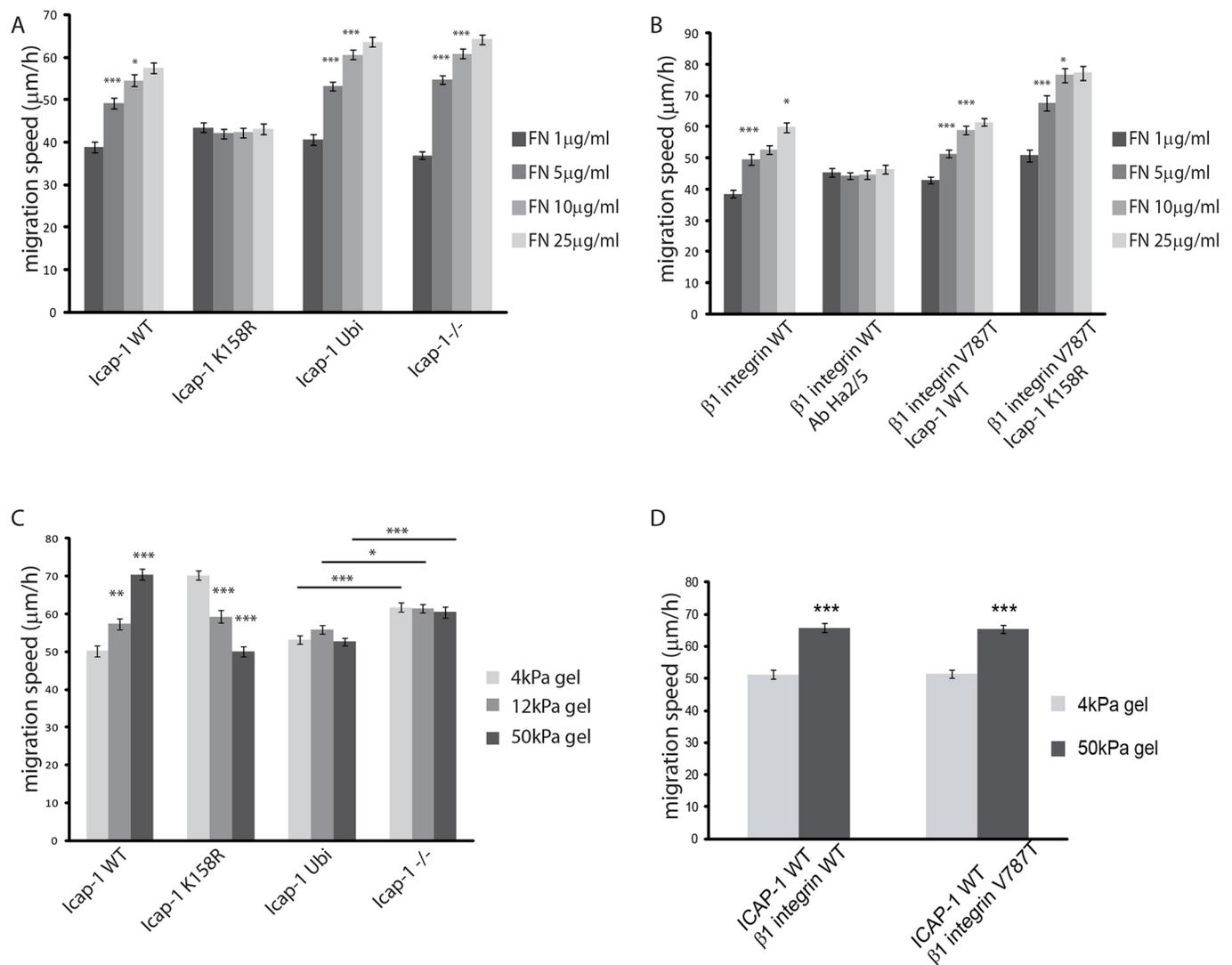
Fig. 3. ICAP-1 ubiquitylation controls FN density and rigidity sensing. Osteoblasts were spread on increasing concentrations of FN and migration was monitored for 5 h using time-lapse microscopy. Cell velocity was determined by individually tracking 150–200 cells from three independent experiments. (A) Cells expressing ICAP-1-WT, the ICAP-1 ubiquitin chimera or cells deficient in ICAP-1 adapted their migratory speed according to the FN density, whereas the cells expressing the ICAP-1 K158R mutant maintained the same speed regardless of the FN density. (B) Similar to the cells expressing ICAP-1 K158R, cells treated with a blocking anti-β1 integrin antibody (Ab Ha2/5) were unable to adapt their migration speed to the FN density. β1 integrin-null cells expressing the β1 integrin mutant that lacks ICAP-1 binding (V787T) were not affected by K158R ICAP-1 expression. (C,D) Osteoblast cells were spread on FN-coated PAA gels of different rigidities. Cell migration was monitored for 5 h using time-lapse microscopy. The cell velocity was determined by individually tracking 150–300 cells in three independent experiments. Similar to in ICAP-1-deficient cells, ICAP-1–Ubi cells did not change their velocity according to gel rigidity whereas WT cells moved more quickly in stiffer gels (C). β1 integrin-null cells expressing the β1 integrin mutant that lacks ICAP-1 binding (V787T) responded to gel rigidity similarly to control cells (D) indicating that the interaction between β1 integrin and ICAP-1 is not necessary to adapt cell migration to substrate stiffness. Error bars indicate the mean±s.e.m. *$P<0.05$, **$P<0.005$, ***$P<0.0005$ (one-way ANOVA and Tukey's HSD test).

We next evaluated the effects of ICAP-1 monoubiquitylation on the ECM rigidity sensitivity. Osteoblast cells (Fig. 3C) or MEF cells (Fig. S3D) infected with ICAP-1 WT, ICAP-1 K158R and ICAP-1–Ubi were plated onto FN-conjugated elastomeric polyacrylamide (PAA) gels with increasing Young's modulus (E) and monitored for cell migration. As expected, the WT ICAP-1 cells moved more quickly on stiffer gels than they did on softer gels (40% increase on the stiffer substrate) (Fig. 3C; Fig. S3D, Movies 5,6). Cells expressing ICAP-1 K158R still responded to the increase in matrix rigidity, whereas cells expressing the monoubiquitylated ICAP-1 displayed a constant migration velocity that was independent of the stiffness of the substrate, like ICAP-1-deficient cells (Fig. 3C; Fig. S3D, Movies 7,8). However, the migration speed of ICAP-1$^{-/-}$

cells was slightly but significantly higher as compared to that of ICAP-1–Ubi cells. This suggests that ICAP-1 monoubiquitylation also controlled the capacity of cells to adapt their velocity to ECM rigidity. As monoubiquitylation prevents ICAP-1 and β1 integrin interaction, we then investigated whether rigidity sensing was dependent on ICAP-1 and β1 integrin interaction. Cells expressing the β1 integrin V787T mutant that are unable to interact with ICAP-1 still adapt their velocity in response to the external rigidity (Fig. 3D) whereas ICAP-1 deficiency led to insensitiveness to substrate stiffness (Fig. 3C). Thus, the presence of ICAP-1 is required even though ICAP-1 interaction with β1 integrin is dispensable for rigidity sensing. Monoubiquitylation of ICAP-1 is a signal that allows the sensing of matrix density and rigidity by

decoupling the inhibitory role of ICAP-1 on β1 integrin from an unexpected role that is independent of its interaction with β1 integrin.

The monoubiquitylation of ICAP-1 increases cell contractility

As rigidity sensing is associated with cell contractility, we sought to determine whether the monoubiquitylated form of ICAP-1 might interfere with cell contractility. First, as a contractility marker, we analyzed the phosphorylation state of myosin light chain (pMLC) by western blotting lysates from WT, and ICAP-1–Ubi and ICAP-1-deficient cells plated onto FN-coated plastic or elastomeric PAA gels with a Young's modulus (E) of 4 or 50 kPa (Fig. S4A). As expected, the level of pMLC in total cell lysates of cells expressing ICAP-1 WT increased with the substrate rigidity. ICAP-1-deficient cells displayed the same behavior as ICAP-1 WT cells. In contrast, cells expressing the monoubiquitylated ICAP-1 showed a constant level of pMLC independently of the rigidity of the substrate. This loss of pMLC regulation is correlated with the inability of ICAP-1–Ubi cells to adapt their velocity to ECM rigidity (Fig. 3C). In addition, an increase of pMLC staining along the stress fibers in ICAP-1–Ubi cells was noted (Fig. 4A). To investigate whether the monoubiquitylated ICAP-1 is involved in the genesis and modulation of forces applied to the substratum, traction force microscopy (TFM) was used. Traction forces generated by the cells were twice as high in ICAP-1–Ubi cells as compared to the WT cells and ICAP-1-deficient cells (Fig. 4B). Therefore, the monoubiquitylation of ICAP-1 increases cell contractility by forcing the phosphorylation of myosin independently of the substrate rigidity.

The monoubiquitylation of ICAP-1 drives MRCKα-mediated cell contractility

Cell contractility relies on the balance between ROCK, MLCK and mDia activities to control elongation and organization of actin filament (Burridge and Wittchen, 2013). To explore the contractility pathways potentially affected by ICAP-1–Ubi, a pharmacological approach was used by testing ROCK, MLCK and mDia inhibitors (Y27632, ML7 and SmifH2, respectively) on the migration of osteoblasts adhered to 4 kPa gels coated with 5 µg/ml of FN. Like WT cells, ICAP-1–Ubi cells migrated slower upon MLCK and mDia inhibition (Fig. S4B). As previously described (Totsukawa et al., 2000), WT cells migrate faster upon ROCK inhibition. In contrast, ICAP-1–Ubi cells were insensitive to Y27632 treatment since no change in migratory speed response was observed as compared with the WT cells (Fig. S4B). This insensitivity to ROCK inhibition in ICAP-1 Ubi cells is not due to the loss of the interaction between ICAP-1–Ubi and β1 integrin since cells expressing the V787T mutant of β1 integrin, which is unable to interact with ICAP-1, are still sensitive to ROCK inhibition (Fig. S4C). Thus, ICAP-1–Ubi cell migration is independent of ROCK-controlled contractility, suggesting an alternative contractile pathway for ICAP-1–Ubi cells.

Besides regulating ROCK1 (Peter et al., 2006), ICAP-1 has been shown to inhibit Cdc42 and Rac1 (Degani et al., 2002), which are involved in the regulation of MRCK. Therefore, we sought to assess whether ICAP-1 could regulate MRCK-dependent cell contractility (Leung et al., 1998). To test this hypothesis, we used a siRNA strategy to knockdown ROCK1, ROCK2, MRCKα and MRCKβ (Fig. 4C,D). The WT ICAP-1 cells moved more quickly on stiffer gels than they did on softer gels whatever the siRNA used except in conditions of ROCK2 deletion suggesting that WT cells adapt their migratory behavior through a ROCK2-dependent contractility and

this behavior is independent of ROCK1, MRCKα and MRCKβ (Fig. 4C). In contrast, only MRCKα silencing in ICAP-1–Ubi cells led to an increase in the cell migration speed when rigidity of the substrate was increased (Fig. 4D). Thus, the cell contractility mode imposed by ICAP-1 monoubiquitylation is dependent on MRCKα and is independent of ROCK1, ROCK2 and MRCKβ. To confirm the involvement of MRCKα in the monoubiquitylated ICAP-1-dependent phosphorylation of myosin, we tested the effect of siRNA against MRCKα or ROCK2 on the decoration of stress fibers by T18/S19 phosphorylated MLC (ppMLC) (Fig. 4E). Whereas the siRNA against ROCK2 decreased the level of ppMLC in WT cells, the depletion of MRCKα significantly reduced the level of ppMLC in cells infected with ICAP-1–Ubi. Thus, ICAP-1 monoubiquitylation favors the phosphorylation of myosin II that is dependent on the activity of MRCKα whereas ROCK2 activity is responsible for the phosphorylation of myosin II in WT cells. Taken together, these results show that ICAP-1 monoubiquitylation allows the switch from ROCK2-mediated to MRCKα-mediated cell contractility.

DISCUSSION

Our data show that monoubiquitylation of ICAP-1, a protein that associates with integrin cytoplasmic domains, by Smurf1 is involved in regulating the balance between adhesion and contractility. ICAP-1 monoubiquitylation inhibits its binding to β1 integrin, subsequently regulating the number and organization of β1 integrin-containing FAs. ICAP-1 and its monoubiquitylated form may be crucial mediators involved in the balance between ROCK2 and MRCKα activities in order to adapt cell contractility to the variability of ECM stiffness. Our results show that these two functions of ICAP-1 are integrated by the cell to sense both matrix density and rigidity.

Smurf1 as a node to control focal adhesion dynamics and cell contractility

In addition to its ability to ubiquitylate talin (Huang et al., 2009), Smurf1 was a good candidate for ICAP-1 monoubiquitylation because Smurf1 associates with the cerebral cavernous malformations (CCM) complex (Crose et al., 2009), which interacts with ICAP-1 (Hilder et al., 2007). Smurf1 also possesses an NPxY motif that might be able to interact with ICAP-1 phosphotyrosine-binding (PTB) domain. Smurf1 is also involved in cell polarity and cell migration (Sahai et al., 2007; Wang et al., 2003). We demonstrated that the monoubiquitylation of ICAP-1 by Smurf1 is not involved in ICAP-1 degradation via the proteasome, but rather, regulates the assembly and organization of FAs by modulating the ICAP-1–β1-integrin interaction. The ICAP-1–β1-integrin interface is likely disrupted upon ICAP-1 monoubiquitylation since K158 is in close vicinity to the I138 residue known to be important for the β1 integrin interaction (Chang et al., 2002; Liu et al., 2013).

In addition to their canonical roles in cell growth and differentiation mediated through TGF signaling (Zhu et al., 1999), accumulating evidence indicates that Smurfs play key roles in regulating cell adhesion and migration. Smurf1 is localized in lamellipodia and filopodia, with a fraction of Smurf1 in FAs (Huang et al., 2009; Wang et al., 2003). Smurf1 ubiquitylates molecules involved in both cell adhesion and contractility. Smurf1 controls talin head degradation, and subsequently adhesion stability and cell migration (Huang et al., 2009). RhoA ubiquitylation by Smurf1 causes its degradation at the leading edge of migrating cells and promotes lamellipodium formation (Sahai et al., 2007; Wang et al.,
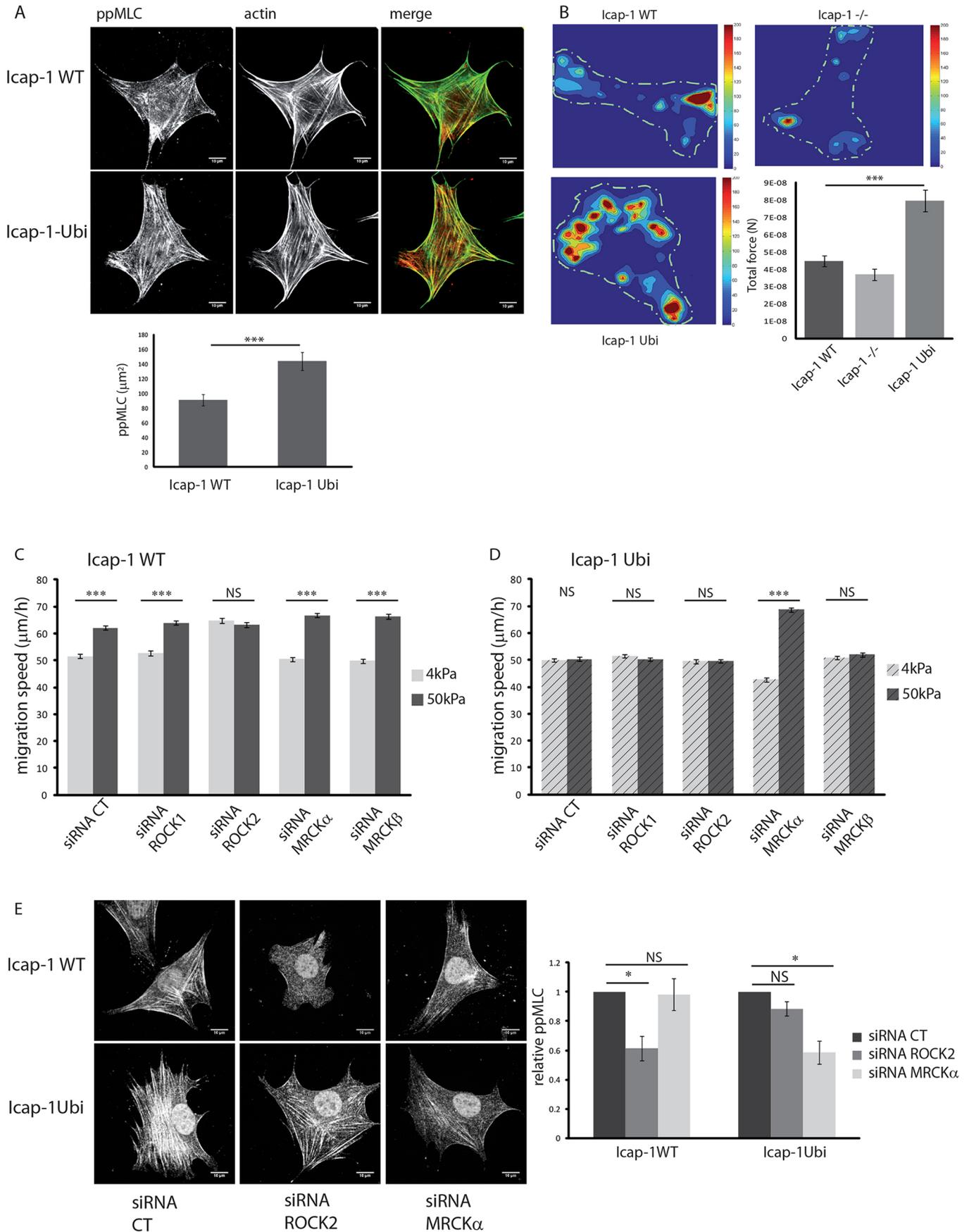
Fig. 4. See next page for legend.

Fig. 4. The monoubiquitylation of ICAP-1 drives an MRCKα-mediated cell contractility. (A) Immunostaining of ppMLC and actin (phalloidin) in WT cells and ICAP-1–Ubi osteoblast cells. Note the increase of ppMLC along the stress fibers as seen from the quantification of 80 cells from three independent experiments. (B) Representative traction force maps obtained by TFM in ICAP-1 WT, ICAP-1-deficient and ICAP-1–Ubi osteoblast cells (images). TFM experiments showed an increase of the force applied on the substrate in ICAP-1–Ubi cells as compared to ICAP-1 WT and ICAP-1-deficient cells (n=78 from three independent experiments) (graph). Error bars indicate the mean±s.e.m. ***P<0.0005 (one-way ANOVA and Tukey's HSD test). (C) Osteoblasts were spread on FN-coated PAA gels of different rigidities. Cell migration was monitored for 5 h using time-lapse microscopy. Cell velocity was determined by individually tracking 200–300 cells in three independent experiments. Monitoring of WT cells migration after treatment with scrambled siRNA (siRNA CT) or siRNA against ROCK1, ROCK2, MRCKα or MRCKβ on 4 or 50 kPa gels. Note that WT cells are sensitive to ROCK2 siRNA treatment. (D) Monitoring of ICAP-1–Ubi osteoblast cells migration after treatment with scrambled siRNA (siRNA CT) or with siRNA against ROCK1, ROCK2, MRCKα or MRCKβ on 4 or 50 kPa gels. Note that ICAP-1–Ubi cells are sensitive to MRCKα siRNA treatment. (E) Immunostaining of ppMLC in WT osteoblast cells and ICAP-1–Ubi osteoblast cells after treatment with siRNA against ROCK2 or MRCKα (left panel). The right-hand panel shows a quantification of ppMLC staining. Note the decrease of ppMLC staining along the stress fibers after siRNA against ROCK2 for the WT cells whereas the decrease of ppMLC is observed after treatment with siRNA against MRCKα for ICAP-1–Ubi cells (n>80). Error bars indicate the mean±s.e.m. *P<0.05; ***P<0.0005; NS, not significant (one-way ANOVA and Tukey's HSD test). Scale bars: 10 μm.

2003). Our data demonstrate that Smurf1 is a node controlling both FA dynamics and cell contractility through a common target, ICAP-1. ICAP-1 monoubiquitylation not only regulates the number and organization of β1 integrin-containing FAs but also inhibits ROCK signaling and promotes the MRCK signaling pathway. Therefore, we add another piece of evidence showing that the RhoA–ROCK pathway is inhibited by Smurf1, and we demonstrate for the first time that Smurf1 controls a switch from a ROCK-dependent to a MRCK-dependent cell contractility.

The monoubiquitylation of ICAP-1 as a switch from ROCK2-mediated to MRCKα-mediated contractility

In addition to its role in the β1 integrin activation cycle (Millon-Frémillon et al., 2008), ICAP-1 interferes with small GTPase signaling and cell contractility by putting a cap on RhoA activation (Faurobert et al., 2013) and inhibiting Rac1 and Cdc42 (Degani et al., 2002). So far, how ICAP-1 can regulate both RhoA–ROCK signaling and the Cdc42 and Rac1 pathway was unclear. It has been described that a cooperation between RhoA–ROCK and Cdc42 or Rac1–MRCK signaling can control cell contractility cell polarity, morphology and morphogenesis (Gally et al., 2009; Unbekandt and Olson, 2014; Wilkinson et al., 2005). Their respective contribution might depend on ECM rigidity. ICAP-1, independently of its

interaction with β1 integrin, could act as a sensor of ECM rigidity differently modulating the activity of each enzyme depending on the substrate stiffness. It could act by playing on the level of activation of RhoA, Rac1 or Cdc42 and by directly modulating the activity of ROCK2 and MRCKα. Thus, we propose that ICAP-1 monoubiquitylation by Smurf1 is a key event leading to a switch from ROCK2-mediated to MRCKα-mediated cell contractility. ICAP-1 and its monoubiquitylated form regulate ROCK2- and MRCKα-dependent MLC phosphorylation independently of interaction with β1 integrin. This is in line with previous studies, which do not attribute a major role of β1 integrin to ECM rigidity sensing (Jiang et al., 2006). Taken together, our results show that ICAP-1 contributes to an elaborate signaling network responsible for maintaining cell tensional homeostasis, going from the dynamics of cell adhesion to the adaptation of contractile actomyosin machinery. ICAP-1 may function in β1 integrin-dependent and -independent pathways to orchestrate both the chemo and mechanical regulation of cell migration. These two pathways might regulate distinct signaling cascades through a switch operated by Smurf1 to adapt the cellular migratory response (Fig. 5). ICAP-1 is essential in rigidity sensing and its monoubiquitylation might be crucial for the adaptation of cells to a local variation of ECM stiffness in tissues or a change of ECM composition during development or in pathological situations. ICAP-1 monoubiquitylation would allow the cell to adapt its the contractility depending on substrate stiffness by controlling the balance between ROCK2-and MRCKα-mediated cell contractility. In future studies, it will be important to identify the factors that are regulated by ICAP-1 independently of its interaction with β1 integrin in order to develop a more complete understanding of the functions of ICAP-1 in mechanosensing.

MATERIALS AND METHODS
Plasmid construction
The plasmids pCMVFlag-Smurf1 WT, pGEX4T1-Smurf1 WT, pGEX4T1-Smurf2 WT, pRK5-Myc-Smurf1 and pRK5-HA-Ubiquitin-WT were obtained from Addgene (Cambridge, MA; numbers 11752, 13502, 13504, 13676 and 17608). pGEX4T1 plasmids containing the β1 or β3 integrin cytoplasmic domain, as well as pCLMFG retroviral vectors containing WT β1 integrin or the V787T mutant, have been previously described (Brunner et al., 2011). The pSG5-ubiquitin-His vector was a kind gift from Saadi Khochbin (U823 INSERM-UJF, Grenoble, France). The full-length cDNA of WT human ICAP-1 was subcloned into the *Eco*RI and *Bam*HI sites of the pBabe-puro retroviral vector (pBabe-ICAP-1 WT). The K158R substitution was introduced into the ICAP-1 cDNA via site-directed mutagenesis (pBabe-ICAP-1 K158R). The Myc tag was inserted at the 3′ end of the ICAP-1 or ubiquitin cDNA using PCR. The Myc-tagged ICAP-1 cDNA was subcloned between the *Bam*HI and *Eco*RI sites of the pcDNA3.1 expression vector and mutated to generate the K158R mutant.
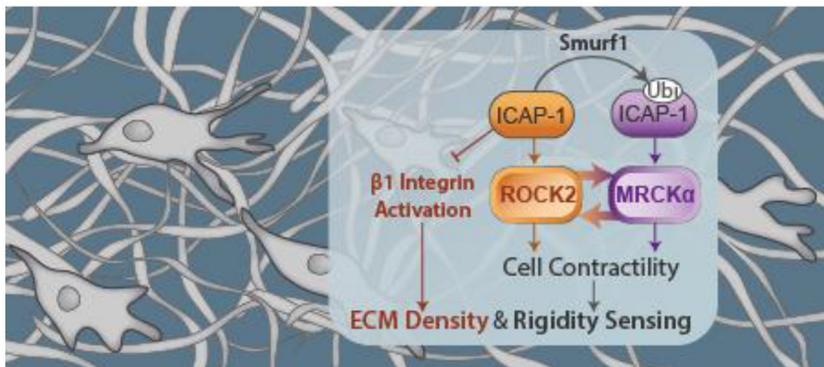

Fig. 5. A ROCK2–MRCKα switch operated through the monoubiquitylation of ICAP-1 by Smurf1 to adapt the cellular migratory response. Smurf1 is able to monoubiquitylate ICAP-1. The monoubiquitylation of ICAP-1 by Smurf1 is required to release inhibitory effect of ICAP-1 on β1 integrin, thereby facilitating the activation–deactivation cycle of β1 integrin important for ECM density sensing and adaptive cell migration responses. The monoubiquitylation of ICAP-1 allows the switch from ROCK2-mediated to MRCKα-mediated cell contractility to control ECM rigidity sensing.

The cDNA of Myc-tagged ubiquitin was amplified and inserted at the 3′ end of the ICAP-1 cDNA, between the EcoRI and XhoI sites of the pcDNA3.1 vector (pcDNA3.1-ICAP-1-myc, pcDNA3.1-ICAP-1 K158R-myc and pcDNA3.1-ICAP-1-Ubi-myc). The ICAP-1-Ubi-myc cDNA was subcloned into the pBabe-puro, between the BamHI and SalI sites (pBabe-ICAP-1-Ubi-myc).

Cell culture, transfection and antibodies
Immortalized osteoblasts were cultured in Dulbecco's modified Eagle's medium (DMEM; Invitrogen, Life Technologies, Cergy Pontoise, France), CHO cells and HeLa cells were grown in αMEM (PAA) at 37°C in a humidified, 5% CO_2 chamber. All media are supplemented with 10% fetal calf serum (FCS; Invitrogen), 100 U/ml penicillin and 100 μg/ml streptomycin. Immortalized osteoblasts from $icap-1^{-/-}$; $Itgb1^{flox/flox}$ mice were generated as previously described (Bouvard et al., 2007). These cells were treated with or without adenoCre viruses obtained from the gene transfer vector core (University of Iowa) to generate β1 integrin-null cells. The ICAP-1-null cells were incubated with or without retroviral particles to obtain rescued cells expressing ICAP-1 WT, ICAP-1 K158R or the ICAP-1–Ubi chimera. The cells were selected with 1 mg/ml puromycin to produce cell populations with heterogeneous ICAP-1 expression levels. β1 integrin-null cells that had already been rescued with ICAP-1 were again infected with retrovirus to obtain double-rescued cells expressing ICAP-1 (WT or mutant) and WT β1 integrin or the V787T mutant. For all experiments, cells were trypsinized and washed in PBS before plating in DMEM containing 4% FN-free FCS for 3 h. Osteoblasts ($90×10^4$ cells) were transfected with 25 pmol siRNA and 6 μl Lipofectamine RNAiMAX reagent (Invitrogen) according to the manufacturer's instructions. The cells were used 2 days after transfection. SMARTpool siRNA (Dharmacon Research Inc., Lafayette, LA) was used against appropriate proteins, along with the control siRNA sequence 5′-AGGUAGUGUAAUCGCCUUG-3′. HeLa cells were transfected with control or Smurf1 siRNA SMARTpool siRNA (Dharmacon Research Inc.) using Lipofectamine RNAiMAX (Invitrogen) according to the manufacturer's instructions; two rounds of transfection were performed. ICAP-1 and His-tagged ubiquitin were overexpressed using Fugene (BD Biosciences, Le Pont de Claix, France) according to the manufacturer's instructions. CHO cells were transfected with ExGen (EUROMEDEX, Souffelweyersheim, France) following the manufacturer's instructions using pcDNA3.1-ICAP-1-myc, pcDNA3.1-ICAP-1K158R-myc or pcDNA3.1-ICAP-1-Ubi-myc. CHO cells were cotransfected with pcDNA3.1-ICAP-1-myc or pcDNA3.1-ICAP-1 K158R-myc and pSG5-ubiquitin-His. After 24 h, the transfected cells were incubated with the proteasome inhibitor MG132 (20 μM) for 4 h. The antibodies used in this study were the following: rat anti-β1 integrin 9EG7 (1:100; BD Biosciences, 553715), donkey anti-rabbit-IgG conjugated to HRP (1:12,000; Jackson ImmunoResearch, UK, 711-036-152), goat anti-rat-IgG conjugated to Alexa Fluor 488 (1:1000; Invitrogen, A-11006), mouse anti-actin (1:1000; Sigma-Aldrich, Saint Quentin Fallavier, France, A2066), mouse anti-Smurf1 (1:1000; Santa Cruz Biotechnology, Heidelberg, Germany, Sc-100616) rabbit anti-T18/S19 MLC [1:1000 (western blotting) or 1:100 (immunofluoresence); Cell Signaling Technology, Leiden, The Netherlands], and rabbit anti-ICAP-1 (1:1000; Millon-Frémillon et al., 2008).

Purification of His-tagged ubiquitylated proteins
Transfected CHO cells were lysed in phosphate-buffered saline (PBS) containing 10% glycerol, 0.3% NP40, 5 mM NEM, 10 mM NaF, phosphatase inhibitor cocktails 2 and 3 (Sigma-Aldrich), and a protease inhibitor cocktail (cOmplete, EDTA-free, Roche, Meylan, France). After centrifugation (15,000 g for 20 min), the supernatants were incubated with Talon Metal Affinity resin (Clontech, Saint Germain en Laye, France) for 2 h. After three washes, the proteins were eluted in Laemmli buffer and analyzed by western blotting (3% of the total lysate is used for the input track).

Pulldown assays
GST–Smurf1 and GST–Smurf2 were expressed in E. coli (BL21 DE3 RIL) as previously described (Wang et al., 2006). Transfected CHO cells were lysed in buffer containing 50 mM Tris-HCl pH 7.7, 150 MG132, protease

inhibitor cocktail and phosphatase inhibitor cocktails 2 and 3. The supernatants were incubated for 3 h with GST–Smurf1-, GST–Smurf2- or GST-coupled glutathione–Sepharose beads. After five washes in lysis buffer, the samples were eluted in Laemmli buffer and analyzed by western blotting (3% of the total lysate is used for the input track). GST–β1-integrin and GST–β3-integrin were expressed in E. coli (BL21 DE3 RIL), and pulldown experiments with supernatants from transfected CHO cells were performed as previously described (Brunner et al., 2011).

ICAP-1 protein lifetime measurement
Transfected CHO cells were incubated with 100 μg/ml cycloheximide (Sigma-Aldrich) with or without 20 μM MG132. Cells were lysed in RIPA buffer at the indicated times, and the protein concentration was measured using the BCA assay. Total proteins (20 μg) were separated by SDS-PAGE and immunoblotted as below.

Flag immunoprecipitation
Transfected CHO cells were lysed in lysis buffer (50 mM NaCl, 10 mM Pipes, 150 mM sucrose, 50 mM NaF, 40 mM $Na_4P_2O_7·10H_2O$, 1 mM Na_3VO_4, pH 6.8, 0.5% Triton X-100, 0.1% sodium deoxycholate, and protease inhibitor cocktail). The supernatants were incubated for 1 h with anti-Flag M2 magnetic beads (Sigma-Aldrich). After four washes with lysis buffer, the samples were eluted in lysis buffer containing 100 μg/ml Flag peptide (Sigma-Aldrich) and analyzed by western blotting (3% of the total lysate is used for the input track).

ELISA assay
The interaction between recombinant ICAP-1 and ICAP-1–Ubi was analyzed using a solid-phase assay. Briefly, a 96-well tray (MaxiSorp, Nunc) was coated with either ICAP-1-His or ICAP-1–Ubi–His (40 μg/ml) for 16 h at 4°C and blocked with 3% BSA in PBS for 1 h at room temperature. Increasing concentrations of GST, the GST–β1-integrin cytoplasmic domain or GST–Smurf1 were added for 1 h. After three washes in PBS with 0.1% Tween20, detection of bound proteins was performed by using the antibodies directed against β1 integrin cytoplasmic domain or Smurf1. Nonspecific binding to BSA-coated wells was subtracted from the results as background.

pMLC western blot analysis
Cells were plated on plastic or on PAA gels with controlled rigidities of 50 kPa or 4 kPa (Cell Guidance System, Cambridge, UK) coated with 1 μg/cm^2 (5 μg/ml) of FN. The next day cells were lysed in Laemmli buffer and analyzed by western blotting. Immunoblots were visualized using the ECL system (Biorad) and Chemidoc imaging system (Biorad).

Traction force microscopy
The PAA substrates were prepared on two-well LabTek slides (Thermo Fischer Scientific, Ulm, Germany) using 8% acrylamide mixed with appropriate percentage of bis-acrylamide and 10 mM HEPES (pH 8.5) gels. After two Sulfo-SANPAH (Thermo Fischer Scientific, Ulm, Germany) activations, the gels were coated with 5 μg/ml FN (1 μg/cm^2) at 4°C overnight. We used a concentration of 0.15% of bis-acrylamide to create gels with controlled rigidities of 5 kPa. Cells were plated at an approximate density of $2×10^4$ cells per cm^2 for 3-4 h and images were acquired on an iMIC Andromeda (FEI, Gräfelfing, Germany) microscope at 40x magnification. Force calculations were performed as previously described (Tseng et al., 2011).

Random migration analysis
Cells were plated on a 12-well plate containing a PAA substrate (Cell Guidance System) or on an 8-well LabTek slide coated with various FN concentrations at an approximate density of $1.2×10^5$ per cm^2 for 3 h in CO_2-independent DMEM containing 4% FN-free FCS. The cells were maintained at 37°C and imaged on an inverted microscope (Zeiss Axiovert 200) equipped with a motorized stage, cooled CCD camera (CoolSnap HQ2, Roper Scientific) and a 10× objective (EC Plan-Neofluar) for live-cell imaging for 5 h at a frequency of 1 image every 4 min. Inhibitors were added as indicated to the medium 10 min prior to the initiation of image acquisition and maintained throughout the migration assay at a final

concentration of 10 μM for Y27632 (Calbiochem), 5 μM for ML7 (Calbiochem) and 2 μM for SmifH2 (Calbiochem). Cell velocity was obtained using the manual tracking plug-in in ImageJ software. A total of 150–300 cells were analyzed from at least five different locations in each experiment, and results were collected from three independent experiments.

Immunofluorescence

Cells were plated at an approximate density of 2×10^4 cells per cm^2 for 2.5 h in 24-well plates on slides coated with 0.6 μg/cm^2 (2 μg/ml) or 1.5 μg/cm^2 (5 μg/ml) of FN in DMEM containing 5% FN-depleted serum; the cells were then fixed and immunostained as previously described (Millon-Fremillon et al., 2008). For the focal adhesion analysis, images were acquired on an Axio Imager (Zeiss) microscope at with a 63× objective. We analyzed the β1 integrin staining of 30–40 cells from two independent experiments using a thresholding method and the particle analyzer in ImageJ. Particles larger than 0.5 $μm^2$ were analyzed. Internal focal adhesions are defined as a FA that was more than 3 μm distal to the plasma membrane. For the ppMLC-decorated stress fibers, images were acquired on an iMIC Andromeda (FEI) microscope at with a 40× objective. We analyzed the phosphorylation of Thr18 and/or Ser19 on the light myosin chain in 90–100 cells from three independent experiments by using the 'Unsharp mask' and the particle analyzer plug-in in ImageJ software. Objects bigger than 0.5 $μm^2$ were analyzed.

Statistical tests

All data sets were analyzed with R (http://www.R-project.org/). We used an ANOVA-2 analysis and Tukey's HSD post-hoc test when necessary. Results are mean±s.e.m. Significance is indicated with asterisks (*$P<0.05$, **$P<0.005$, ***$P<0.0005$).

Supplementary information

Supplementary information available online at
http://jcs.biologists.org/lookup/doi/10.1242/jcs.200139.supplemental

References

Bouvard, D., Aszodi, A., Kostka, G., Block, M. R., Albigès-Rizo, C. and Fässler, R. (2007). Defective osteoblast function in ICAP-1-deficient mice. *Development* 134, 2615-2625.

Brunner, M., Millon-Frémillon, A., Chevalier, G., Nakchbandi, I. A., Mosher, D., Block, M. R., Albigès-Rizo, C. and Bouvard, D. (2011). Osteoblast mineralization requires {beta}1 integrin/ICAP-1-dependent fibronectin deposition. *J. Cell Biol.* 194, 307-322.

Burridge, K. and Wittchen, E. S. (2013). The tension mounts: stress fibers as force-generating mechanotransducers. *J. Cell Biol.* 200, 9-19.

Carvallo, L., Muñoz, R., Bustos, F., Escobedo, N., Carrasco, H., Olivares, G. and Larraín, J. (2010). Non-canonical Wnt signaling induces ubiquitination and degradation of Syndecan4. *J. Biol. Chem.* 285, 29546-29555.

Chang, D. D., Hoang, B. Q., Liu, J. and Springer, T. A. (2002). Molecular basis for interaction between Icap1 alpha PTB domain and beta 1 integrin. *J. Biol. Chem.* 277, 8140-8145.

Chen, C., Tao, T., Wen, C., He, W.-Q., Qiao, Y.-N., Gao, Y.-Q., Chen, X., Wang, P., Chen, C.-P., Zhao, W. et al. (2014). myosin light chain kinase (MLCK) regulates cell migration in a myosin regulatory light chain phosphorylation-independent mechanism. *J. Biol. Chem.* 289, 28478-28488.

Crose, L. E. S., Hilder, T. L., Sciaky, N. and Johnson, G. L. (2009). Cerebral cavernous malformation 2 protein promotes Smad ubiquitin regulatory factor 1-mediated RhoA degradation in endothelial cells. *J. Biol. Chem.* 284, 13301-13305.

Degani, S., Balzac, F., Brancaccio, M., Guazzone, S., Retta, S. F., Silengo, L., Eva, A. and Tarone, G. (2002). The integrin cytoplasmic domain-associated protein ICAP-1 binds and regulates Rho family GTPases during cell spreading. *J. Cell Biol.* 156, 377-387.

Discher, D. E., Janmey, P. and Wang, Y. L. (2005). Tissue cells feel and respond to the stiffness of their substrate. *Science* 310, 1139-1143.

Engler, A. J., Sen, S., Sweeney, H. L. and Discher, D. E. (2006). Matrix elasticity directs stem cell lineage specification. *Cell* 126, 677-689.

Faurobert, E., Rome, C., Lisowska, J., Manet-Dupé, S., Boulday, G., Malbouyres, M., Balland, M., Bouin, A.-P., Kéramidas, M., Bouvard, D. et al. (2013). CCM1-ICAP-1 complex controls β1 integrin-dependent endothelial contractility and fibronectin remodeling. *J. Cell Biol.* 202, 545-561.

Gally, C., Wissler, F., Zahreddine, H., Quintin, S., Landmann, F. and Labouesse, M. (2009). Myosin II regulation during C. elegans embryonic elongation: LET-502/ ROCK, MRCK-1 and PAK-1, three kinases with different roles. *Development* 136, 3109-3119.

Hilder, T. L., Malone, M. H., Bencharit, S., Colicelli, J., Haystead, T. A., Johnson, G. L. and Wu, C. C. (2007). Proteomic identification of the cerebral cavernous malformation signaling complex. *J. Proteome Res.* 6, 4343-4355.

Huang, C., Rajfur, Z., Yousefi, N., Chen, Z., Jacobson, K. and Ginsberg, M. H. (2009). Talin phosphorylation by Cdk5 regulates Smurf1-mediated talin head ubiquitylation and cell migration. *Nat. Cell Biol.* 11, 624-630.

Jégou, A., Carlier, M.-F. and Romet-Lemonne, G. (2013). Formin mDia1 senses and generates mechanical forces on actin filaments. *Nat. Commun.* 4, 1883.

Jiang, G., Huang, A. H., Cai, Y., Tanase, M. and Sheetz, M. P. (2006). Rigidity sensing at the leading edge through alphavbeta3 integrins and RPTPalpha. *Biophys. J.* 90, 1804-1809.

Leung, T., Chen, X.-Q., Tan, I., Manser, E. and Lim, L. (1998). Myotonic dystrophy kinase-related Cdc42-binding kinase acts as a Cdc42 effector in promoting cytoskeletal reorganization. *Mol. Cell. Biol.* 18, 130-140.

Liu, W., Draheim, K. M., Zhang, R., Calderwood, D. A. and Boggon, T. J. (2013). Mechanism for KRIT1 release of ICAP1-mediated suppression of integrin activation. *Mol. Cell* 49, 719-729.

Lu, K., Yin, X., Weng, T., Xi, S., Li, L., Xing, G., Cheng, X., Yang, X., Zhang, L. and He, F. (2008). Targeting WW domains linker of HECT-type ubiquitin ligase Smurf1 for activation by CKIP-1. *Nat. Cell Biol.* 10, 994-1002.

Lu, K., Li, P., Zhang, M., Xing, G., Li, X., Zhou, W., Bartlam, M., Zhang, L., Rao, Z. and He, F. (2011). Pivotal role of the C2 domain of the Smurf1 ubiquitin ligase in substrate selection. *J. Biol. Chem.* 286, 16861-16870.

Millon-Frémillon, A., Bouvard, D., Grichine, A., Manet-Dupé, S., Block, M. R. and Albiges-Rizo, C. (2008). Cell adaptive response to extracellular matrix density is controlled by ICAP-1-dependent beta1-integrin affinity. *J. Cell Biol.* 180, 427-441.

Montanez, E., Ussar, S., Schifferer, M., Bösl, M., Zent, R., Moser, M. and Fässler, R. (2008). Kindlin-2 controls bidirectional signaling of integrins. *Genes Dev.* 22, 1325-1330.

Moore, S. W., Roca-Cusachs, P. and Sheetz, M. P. (2010). Stretchy proteins on stretchy substrates: the important elements of integrin-mediated rigidity sensing. *Dev. Cell* 19, 194-206.

Peter, J. M. S., Belén, A., Jacco van, R., Yvonne, M. W., Dirk, G., Kees, J., Ed, R., Stroeken, P. J., Alvarez, B., Van Rheenen, J. et al. (2006). Integrin cytoplasmic domain-associated protein-1 (ICAP-1) interacts with the ROCK-I kinase at the plasma membrane. *J. Cell. Physiol.* 208, 620-628.

Raab, M., Swift, J., Dingal, P. C. D. P., Shah, P., Shin, J.-W. and Discher, D. E. (2012). Crawling from soft to stiff matrix polarizes the cytoskeleton and phosphoregulates myosin-II heavy chain. *J. Cell Biol.* 199, 669-683.

Sahai, E., Garcia-Medina, R., Pouysségur, J. and Vial, E. (2007). Smurf1 regulates tumor cell plasticity and motility through degradation of RhoA leading to localized inhibition of contractility. *J. Cell Biol.* 176, 35-42.

Schaefer, A., Nethe, M. and Hordijk, P. L. (2012). Ubiquitin links to cytoskeletal dynamics, cell adhesion and migration. *Biochem. J.* 442, 13-25.

Su, Y.-T., Gao, C., Liu, Y., Guo, S., Wang, A., Wang, B., Erdjument-Bromage, H., Miyagi, M., Tempst, P. and Kao, H.-Y. (2013). Monoubiquitination of filamin B regulates vascular endothelial growth factor-mediated trafficking of histone deacetylase 7. *Mol. Cell. Biol.* 33, 1546-1560.

Torrino, S., Visvikis, O., Doye, A., Boyer, L., Stefani, C., Munro, P., Bertoglio, J., Gacon, G., Mettouchi, A. and Lemichez, E. (2011). The E3 ubiquitin-ligase HACE1 catalyzes the ubiquitylation of active Rac1. *Dev. Cell* 21, 959-965.

Totsukawa, G., Yamakita, Y., Yamashiro, S., Hartshorne, D. J., Sasaki, Y. and Matsumura, F. (2000). Distinct roles of ROCK (Rho-kinase) and MLCK in spatial regulation of MLC phosphorylation for assembly of stress fibers and focal adhesions in 3T3 fibroblasts. *J. Cell Biol.* 150, 797-806.
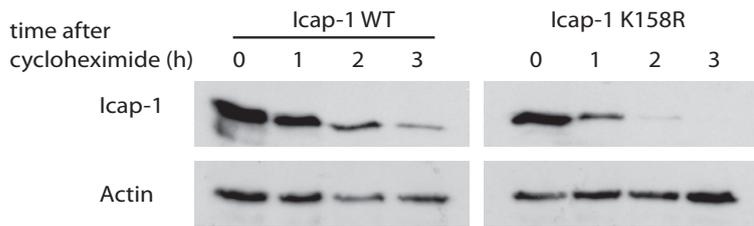
Totsukawa, G., Wu, Y., Sasaki, Y., Hartshorne, D. J., Yamakita, Y., Yamashiro, S. and Matsumura, F. (2004). Distinct roles of MLCK and ROCK in the regulation of membrane protrusions and focal adhesion dynamics during cell migration of fibroblasts. *J. Cell Biol.* **164**, 427-439.

Tseng, Q., Wang, I., Duchemin-Pelletier, E., Azioune, A., Carpi, N., Gao, J., Filhol, O., Piel, M., Théry, M. and Balland, M. (2011). A new micropatterning method of soft substrates reveals that different tumorigenic signals can promote or reduce cell contraction levels. *Lab. Chip* **11**, 2231-2240.

Unbekandt, M. and Olson, M. F. (2014). The actin-myosin regulatory MRCK kinases: regulation, biological functions and associations with human cancer. *J. Mol. Med.* **92**, 217-225.

Visvikis, O., Lorès, P., Boyer, L., Chardin, P., Lemichez, E. and Gacon, G. (2008). Activated Rac1, but not the tumorigenic variant Rac1b, is ubiquitinated on Lys 147 through a JNK-regulated process. *FEBS J.* **275**, 386-396.

Wang, H.-R., Zhang, Y., Ozdamar, B., Ogunjimi, A. A., Alexandrova, E., Thomsen, G. H. and Wrana, J. L. (2003). Regulation of cell polarity and protrusion formation by targeting RhoA for degradation. *Science* **302**, 1775-1779.

Wang, H.-R., Ogunjimi, A. A., Zhang, Y., Ozdamar, B., Bose, R. and Wrana, J. L. (2006). Degradation of RhoA by Smurf1 ubiquitin ligase. *Methods Enzymol.* **406**, 437-447.

Wilkinson, S., Paterson, H. F. and Marshall, C. J. (2005). Cdc42-MRCK and Rho-ROCK signalling cooperate in myosin phosphorylation and cell invasion. *Nat. Cell Biol.* **7**, 255-261.

Ye, F., Snider, A. K. and Ginsberg, M. H. (2014). Talin and kindlin: the one-two punch in integrin activation. *Front. Med.* **8**, 6-16.

Zhu, H., Kavsak, P., Abdollah, S., Wrana, J. L. and Thomsen, G. H. (1999). A SMAD ubiquitin ligase targets the BMP pathway and affects embryonic pattern formation. *Nature* **400**, 687-693.
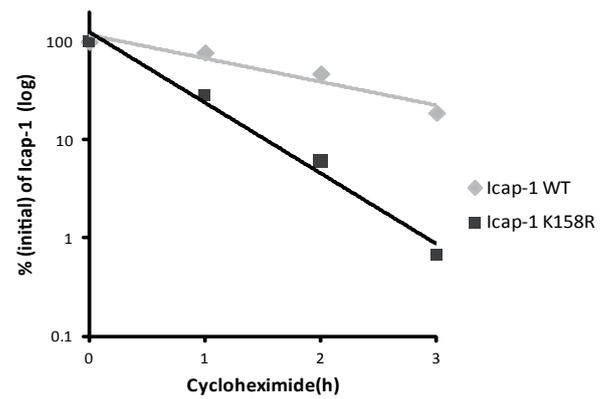
Supplemental information:

Supplemental information includes 4 supplemental figures and 8 supplemental movies.
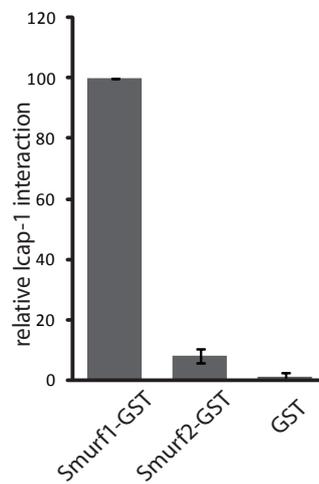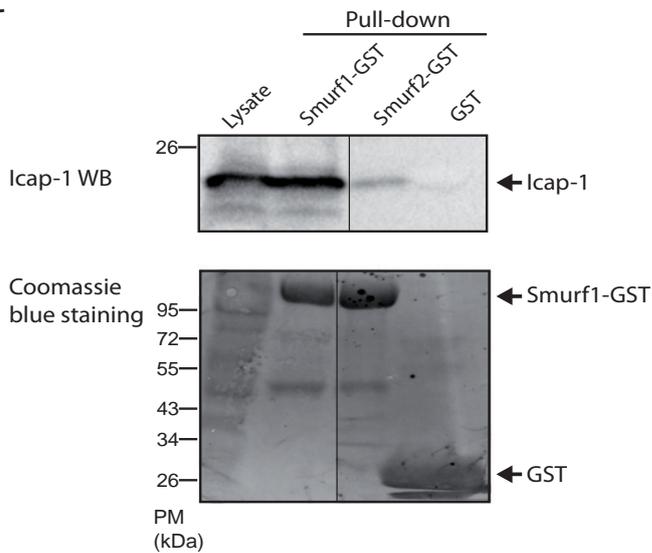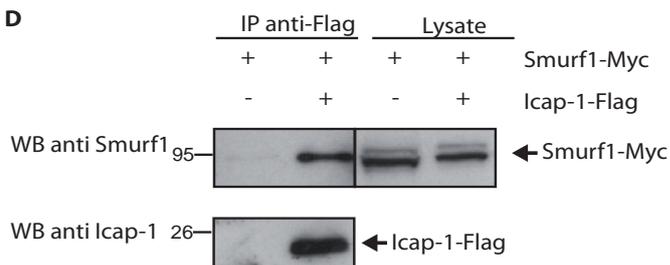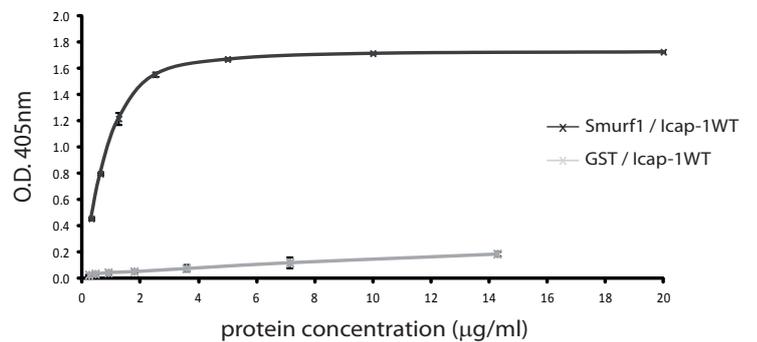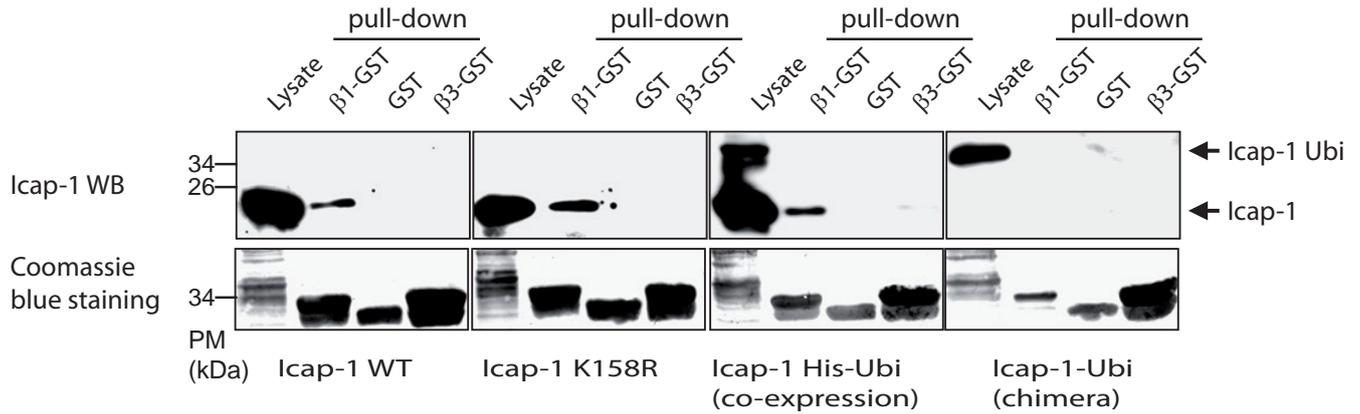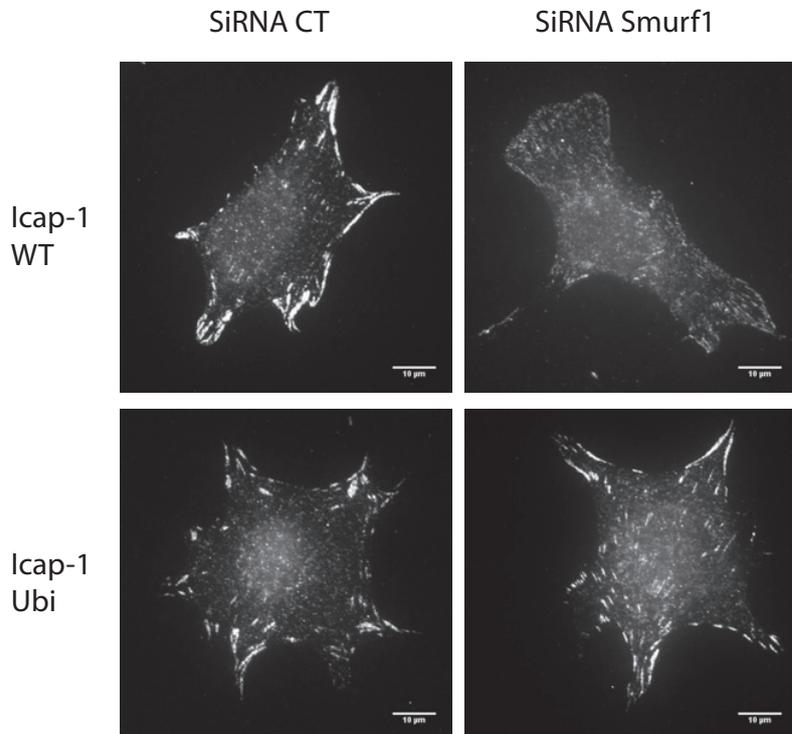
Supplemental figures:

Fig. S1: Monoubiquitination of ICAP-1 by Smurf1 does not lead to ICAP-1 degradation.

A. Cycloheximide was added at t=0 to block protein synthesis. The ICAP-1 protein content in the total lysates was visualized at the indicated times by Western blotting. The results are representative of three independent experiments. B. Quantification of ICAP-1 WT or K158R mutant protein levels over a time-course after the inhibition of protein synthesis. The results are the mean of three independent experiments. C. CHO lysates overexpressing ICAP-1 were incubated with immobilized recombinant Smurf1-GST, Smurf2-GST or GST protein as a control. Interacting protein was analyzed by Western blotting with the anti-ICAP-1 antibody (left panel) and quantified (right panel). The GST protein quantities were controlled using Coomassie blue staining. The results are the mean of two independent experiments. D. Smurf1-myc and ICAP-1-Flag are co-expressed in CHO cells and coimmunoprecipitated with anti-Flag antibodies before blotting against either with anti-Smurf1 or anti-ICAP-1 antibodies. E. Elisa assay showing the direct interaction between Smurf1 and ICAP-1 by using purified recombinant GST-Smurf1 and purified recombinant ICAP-1-His.
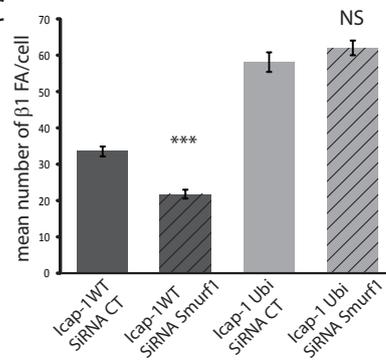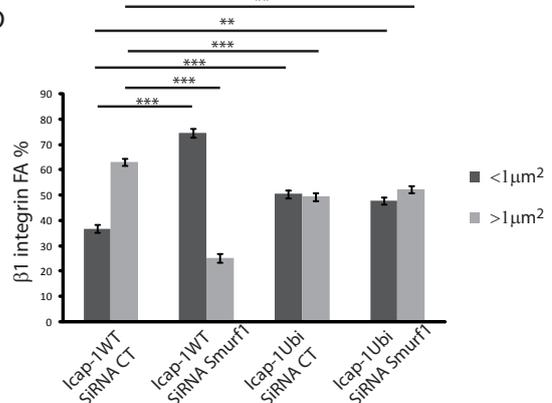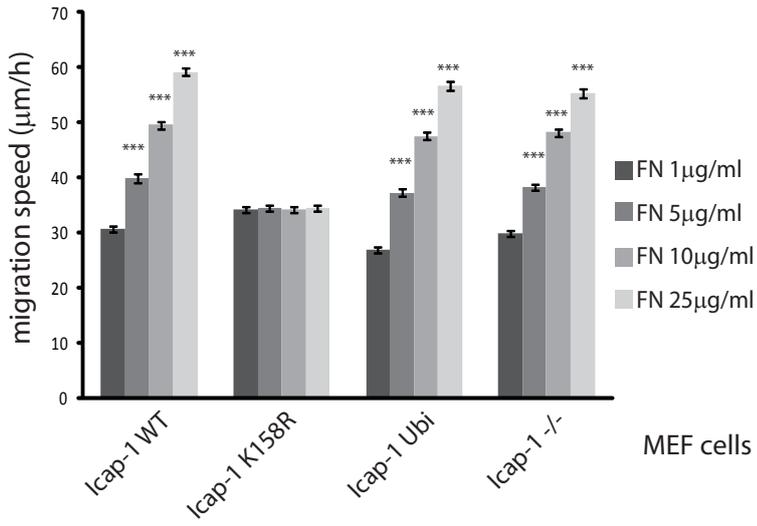
A

B

C

D

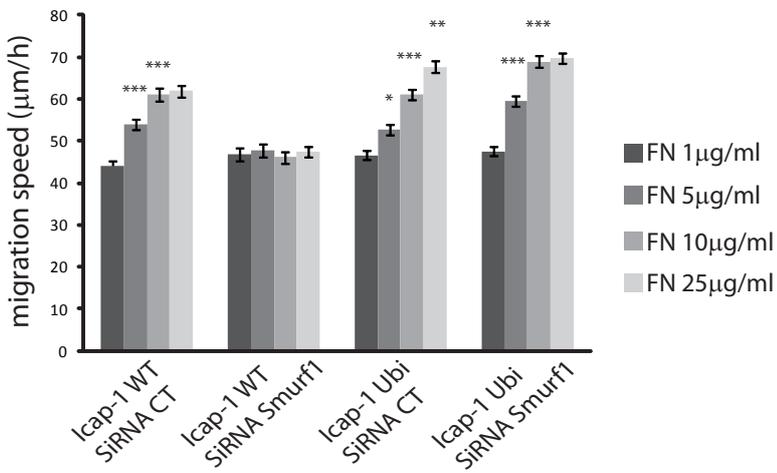**Fig. S2: The deletion of Smurf1 leads to focal adhesion disorganization like ICAP-1 K158R.** A. CHO lysates overexpressing the different ICAP-1 constructs were incubated with immobilized recombinant β1-integrin-tail-GST, β3-integrin-tail-GST or GST protein as a control. The interacting proteins were analyzed by Western blotting with the anti-ICAP-1 antibody. The GST protein quantities were controlled using Coomassie blue staining. The results are representatives of three independent experiments. B. β1 integrin staining of ICAP-1-null osteoblasts rescued with ICAP-1 WT or the ICAP-1 ubiquitin chimera treated with

control or Smurf1 siRNA and spread on FN for 2.5 h. Similar to the cells expressing ICAP-1 K158R, the cells expressing ICAP-1 WT that were treated with Smurf1 siRNA displayed fewer and smaller $\beta 1$ focal adhesions than the cells treated with control siRNA. C. Quantification of the $\beta 1$ integrin focal adhesion number. D. Distribution of the $\beta 1$ integrin focal adhesion areas. Analyses were performed on 30-40 cells from two independent experiments. Error bars indicate SEM. *$p < 0.05$, **$p < 0.005$, ***$p < 0.0005$.
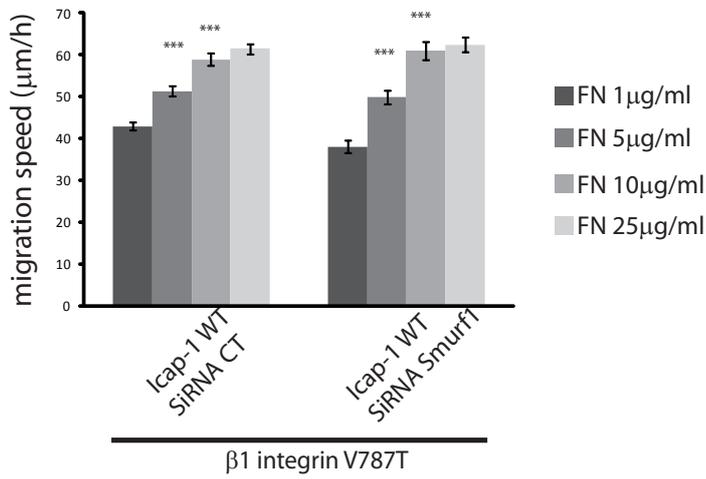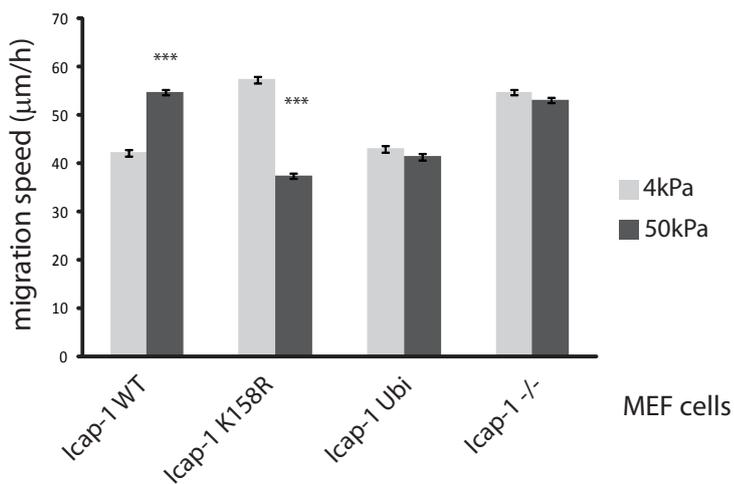
Fig. S3: The deletion of Smurf1 leads to the unresponsiveness of cells to the FN density like ICAP-1 K158R. A. Fibronectin density sensing assay in MEF cells. MEF cells were spread on increasing concentrations of FN and migration was monitored for 5 h using time-lapse microscopy. Cell velocity was determined by individually tracking 150-200 cells from three independent experiments. The cells expressing ICAP-1 WT or the ICAP-1 ubiquitin chimera or cells deficient in ICAP-1 adapted their migratory speed according to the FN density, whereas the cells expressing the ICAP-1 K158R mutant maintained the same speed regardless of the FN density. B. ICAP-1 WT-expressing osteoblast cells that were treated with Smurf1 siRNA were unable to adapt their migratory speed to increasing FN density. This defect was rescued by the ICAP-1 ubiquitin chimera. C. β1 integrin-null osteoblast cells expressing the β1 integrin mutant that lacks ICAP-1 binding (V787T) were not affected by Smurf1 siRNA treatment. D. Rigidity sensing assay in MEF cells. Error bars indicate the mean +/- SEM. $*p< 0.05$, $**p<0.005$, $***p<0.0005$.
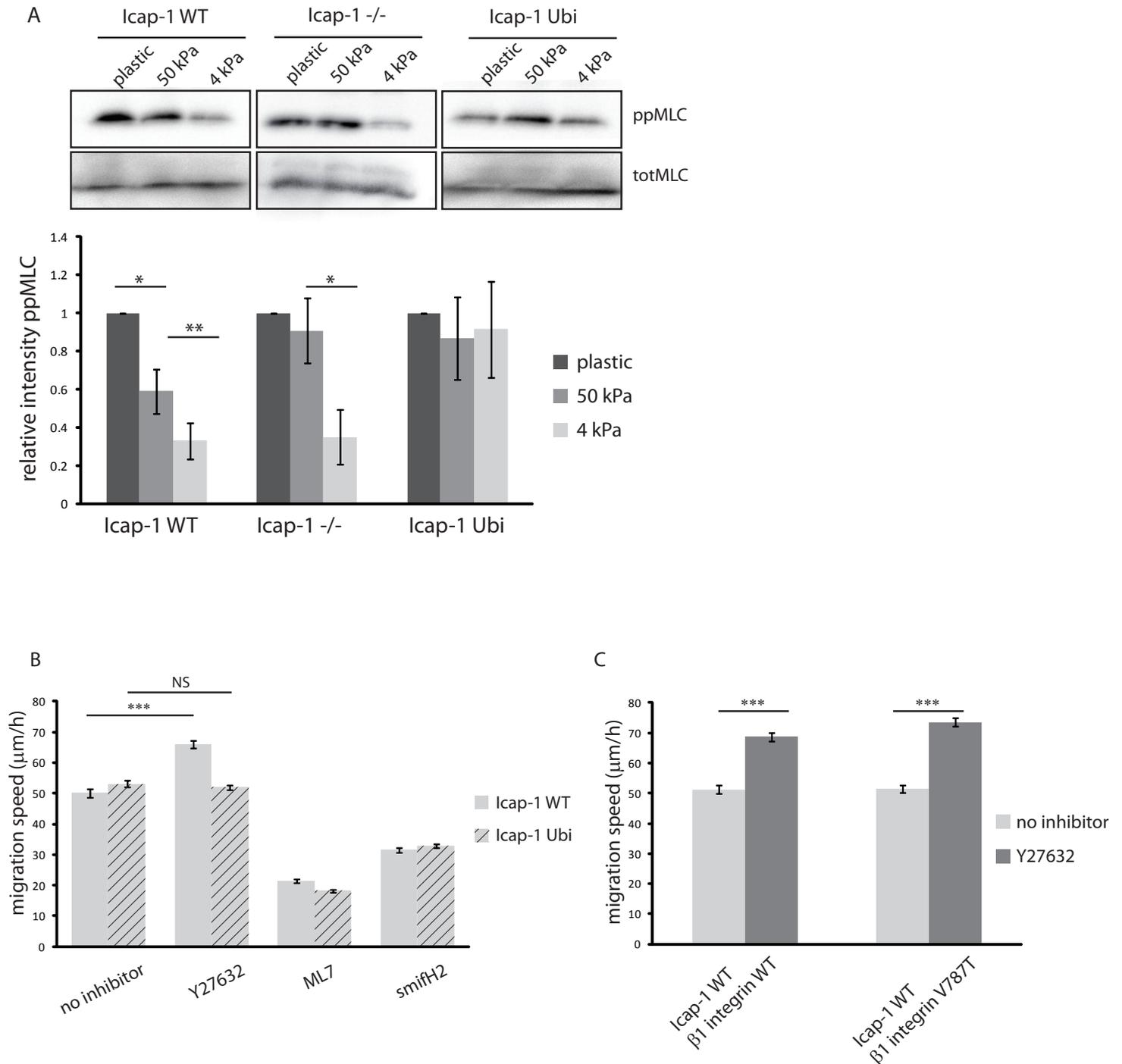
A

B

C

Fig. S4: Identification of contractile pathway in ICAP-1 Ubi osteoblast cells. A. The level of P-myosin is evaluated by western blot in ICAP-1 WT, ICAP-1 deficient and ICAP-1 Ubi cells (upper panel). Note the constant level of P-myosin in ICAP-1 Ubi cells whatever the substrate rigidity after the quantification of the western blot (bottom panel). B. Osteoblasts were spread on FN-coated PAA gels of different rigidities. Cell migration was monitored for 5 h using time-lapse microscopy. Cell velocity was determined by individually tracking of 200-300 cells in three independent experiments to test the effect of inhibitors on WT Osteoblasts cells and osteoblasts transfected with ICAP-1 Ubi cells on 4kPa gels (Y27632: ROCK

inhibitor, 10 μM, ML7: MLCK inhibitor, 5 μM, SmifH2: mDia inhibitor 2 μM). Note that cells expressing ICAP-1 Ubi are insensitive to Y27632. C. β1 integrin-null cells expressing the β1 integrin mutant that lacks ICAP-1 binding (V787T) on 4kPa gels responded to Y27632 treatment in a similar manner to that of the control WT osteoblast cells.

Movie S1: Migration of WT osteoblast cells on 1 µg/ml FN

Movie S2: Migration of WT osteoblast cells on 25 μg/ml FN

Movie S3: Migration of ICAP-1 K158R osteoblast cells on 1 μg/ml FN

Movie S4: Migration of ICAP-1 K158R osteoblast cells on 25 μg/ml FN

Movie S5: Migration of WT osteoblast cells on 4 kPa gel coated with 5 µg/ml FN

Movie S6: Migration of WT osteoblast cells on 50 kPa gel coated with 5 μg/ml FN

Movie S7: Migration of ICAP-1 Ubi osteoblast cells on 4 kPa gel coated with 5 μg/ml FN

Movie S8: Migration of ICAP-1 Ubi osteoblast cells on 50 kPa gel coated with 5 μg/ml FN